DOI:
10.1097/RMR.0000000000000156

Document Version
Peer reviewed version

Topics in Magnetic Resonance Imaging

MR-Guided Cardiac Interventions

--Manuscript Draft--

Manuscript Number:	
Full Title:	MR-Guided Cardiac Interventions
Article Type:	Invited Review Article
Keywords:	MR-Guided Cardiac Interventions Congenital heart disease Electrophysiology Fused Xray and MRI guided catheteristaion
Corresponding Author:	Reza Razavi, M.D. King's College London London, UNITED KINGDOM
Corresponding Author Secondary Information:	
Corresponding Author's Institution:	King's College London
Corresponding Author's Secondary Institution:	
First Author:	Reza Razavi, M.D.
First Author Secondary Information:	
Order of Authors:	Reza Razavi, M.D.
	Kuberan Pushparajah
	Henry Chubb
Order of Authors Secondary Information:	
Manuscript Region of Origin:	UNITED KINGDOM
Abstract:	MR-Guided Cardiac Interventions Diagnostic and interventional cardiac catheterisation is routinely used in the diagnosis and treatment of congenital heart disease. There are well-established concerns regarding the risk of radiation exposure to patients and staff, particularly in children given the cumulative effects of repeat exposure. MRI offers the advantage of being able to provide better soft tissue visualisation, tissue characterisation and quantification of ventricular volumes and vascular flow. Initial work using MRI catheterisation employed fusion of X-ray and MRI techniques, with X-ray fluoroscopy to guide catheter placement and subsequent MRI assessment for anatomical and haemodynamic assessment. Image overlay of 3D previously acquired MRI datasets with live fluoroscopic imaging has also been used to guide catheter procedures. Hybrid X-ray and MRI guided catheterisation paved the way for clinical application and validation of this technique in the assessment of pulmonary vascular resistance and pharmacological stress studies. Purely MRI guided catheterisation also proved possible with passive catheter tracking. First-in-man MRI guided cardiac catheter interventions were possible due to the development of MRI compatible guide-wires, but halted due to guidewire limitations. More recent developments in passive and active catheter tracking have led to improved visualisation of catheters for MRI guided catheterisation. Improvements in hardware and software have also increased image quality and scanning times with better interactive tools for the operator in the MRI catheter suite to navigate through the anatomy as required in real-time. This has expanded to MRI guided electrophysiology studies and radiofrequency ablation in humans. Animal studies show promise for the utility of MRI guided interventional catheterisation. Ongoing investment and

	development of MRI compatible guide-wires have will pave the way for MRI guided diagnostic and interventional catheterisation coming into the mainstream.

Title: MR-Guided Cardiac Interventions

Authors:

Kuberan Pushparajah MD[1,2]

Henry Chubb MBBS, MA[1,2]

Reza Razavi MD[1,2]

1. Division of Imaging Sciences and Biomedical Engineering, King's College London

2. Evelina London Children's Hospital, Guy's and St Thomas' NHS Foundation Trust

Corresponding author:

Reza Razavi

Division of Imaging Sciences and Biomedical Engineering,

King's College London,

Rayne Institute, 4th Floor Lambeth Wing,

St Thomas's Hospital,

Westminster Bridge Road,

London SE1 7EH, The United Kingdom

Email: reza.razavi@kcl.ac.uk

Introduction

Cardiac catheterisation is conventionally guided by fluoroscopy with the inherent concerns of radiation exposure to staff [1-5] and patients. The risk of developing a solid tumour as a result of a single cardiac catheterisation procedure is approximately 1 in 2500 in adults, and 1 in 1000 in children if exposure occurs at 5 years of age[6-9]. The proportion of the body that is irradiated increases as the size of the patient decreases, and some procedures require much longer X-ray exposure and repeat interventions.

The last three decades have seen significant advances in cardiovascular magnetic resonance (CMR), and these advances have supported research into interventional applications using CMR[10-13]. The need for an imaging modality that offers superior structural delineation of complex cardiac anatomy, multiplanar imaging and additional physiologic information, without the risk of ionizing radiation, has allowed CMR guidance of cardiac catheterisation procedures to become a reality. Clinical programs using CMR-guided cardiac catheterization have since developed with promising results.[14-17].

Advantages of CMR

Improved visualization of cardiac anatomy

X-ray-guided cardiac catheterization has poor contrast of soft tissues, such as the heart and great vessels. A skilled operator has to rely on recognizing anatomic structures from previous experience or on contrast angiographic images acquired earlier in the procedure. The lack of adequate visualization increases the risk of perforating the heart or great vessels, especially in complex interventional procedures. Cardiac interventions can involve selection of an appropriate device and

its successful deployment within the heart or great vessels, which requires accurate measurement of the size of defects and nearby anatomic structures. Such measurements can be difficult with X-Ray fluoroscopy (XRF). CMR provides excellent soft tissue visualisation of the cardiac chambers and vessels in 3D whole heart images as well as 2D slices in any plane. Tissue characterisation by CMR also allows targeting a region of interest such as myocardial biopsy in areas of scar [18].

Physiologic information

Conventional cardiac catheterization is also used to obtain functional information. Invasive pressures and blood gases are commonly used to calculate systemic and pulmonary blood flow and resistance. The Fick principle is used to estimate flow, and is dependent on multiple measurements (haemoglobin, aortic/pulmonary artery oxygen saturation, partial pressure, oxygen consumption), which can be a considerable source of inaccuracy. Accuracy is further reduced in patients with large intracardiac shunts and high pulmonary blood flow[19-24].

Velocity encoded phase contrast CMR is a validated technique that enables non-invasive quantification of blood flow in major vessels. Cardiac output and the pulmonary-to-systemic flow ratio (Qp:Qs) measured using this technique have been shown to be accurate[25-31]. This set the path for a novel method of quantification of pulmonary vascular resistance (PVR) in patients with congenital heart disease and or pulmonary hypertension by combining invasive pressure measurements and CMR flow data[32-34]. PVR assessment in this way has been utilised in large clinical case series with good results and is an accepted part of routine clinical practice where it is viewed as a 'gold-standard' [17,35].

Assessment of global and regional ventricular function can also be carried more accurately with cine steady-state free precession (SSFP) cardiovascular MR than with X-ray angiography. Cardiovascular MR does not rely on assumptions about cardiac geometry, unlike with XRF or even echocardiography, which is particularly relevant in CHD.

Combining invasive pressure measurements with CMR-derived blood flow and ventricular volumes opens up interesting new ways of investigating pathophysiology. It allows for the study of pulmonary vascular compliance, derived ventricular pressure-volume loops, and assessment of load-independent ventricular function[36-39]. Pharmacological stress studies have also been applied in CMR/XMR catheter studies to assess haemodynamic responses[39-44].

Using CMR for electrophysiological procedures

CMR-guidance of electrophysiological (EP) procedures presents three fundamental advantages. The first is that of identification and improved targeting of the arrhythmia substrate: CMR has been demonstrated to be capable of delineating the regions of tissue damage and fibrosis that are integral in the instigation and perpetuation of arrhythmias [45,46]. The second is the optimization of intra-procedural guidance with the use of both passive and active tracking techniques, and the imaging of contiguous structures. Finally, the third main advance is the capability for visualization and objective assessment of ablation lesions.

EP substrate identification

Both ventricular and atrial arrhythmogenic substrate have been identified on CMR imaging [47,48], and the implementation of data regarding local myocardial characterization is increasingly used to

guide procedures. Ventricular substrate is generally the more amenable to evaluation by CMR as there is increased wall thickness and higher consequent contrast between healthy and pathological tissue. Ventricular tachycardia (VT) occurs due to scar related re-entry and scar can be accurately visualized using LGE techniques [45,46]. In particular, the scar border zone has been shown to be critical in the perpetuation of the arrhythmia, and its abolition forms the basis of substrate-based VT ablation [49-51].

However, improvements in clinical ablation outcome with the use of CMR-derived substrate information have been modest [52]. Importantly, though, all studies that have used CMR-derived substrate identification to guide ablation have relied upon electroanatomic (EAM) image fusion techniques [53-55]. For this, the imaging is integrated within the EP procedure by matching the shape of the cardiac chambers between the EAM system (derived from tracking all the recorded positions of a cardiac catheter within an operator-defined space) and the imaging. Registration errors are significant and include discrepancies in landmark identification, cardiac chamber conformational changes (arising from differing loading conditions and tachyarrhythmias), and translational changes (due to patient movement, cardiac motion and respiratory motion). CMR-derived targets may be typically 2-4mm wide for VT ablation [56] and even less for atrial ablation [54,57]. Small errors in registration mean that either a very broad region must be ablated or critical targets are left untouched, with consequent impact on safety, time and efficacy.

EP Lesion imaging

Real-time imaging

The real-time imaging of ablation lesions, during energy application, has the nearly unique potential to enable to titration of energy application to ensure transmural lesions. Steiner et al first demonstrated the technical feasibility of real-time in-vivo MR-imaging of RF lesion formation for a swine paraspinal muscle ablation [58]. However, there is only a small body of literature that has demonstrated real-time MR imaging of cardiac lesion formation as clearly it can only be performed for MR-guided EP procedures, and relatively few studies have focused upon this aspect of research [59-61] . The work of the Bordeaux group is particularly promising [61], and implementation within a real-time interface appears to be feasible in the near future.

Acute lesion imaging (<4hours)

There is a great deal more evidence for acute imaging of ablation lesions, but the sensitivity and specificity of acute lesion imaging for prediction of chronic lesion formation remains controversial. Furthermore, much of the data on human ablation relates to imaging at 24 hours post ablation, which is not a clinically useful time interval. Imaging needs to be performed at the same procedure in order to guide further ablation, and therefore a maximum time interval of around 4 hours post-ablation is considered applicable for intra-procedural acute imaging.

In animal models, it has long been established that ventricular lesions can be visualized immediately following ablation [62]. Detailed delineation of the pharmacokinetics of Gad within acute RF injury lesions [63] has been performed, and has been correlated with non-enhanced sequences such as T2-weighted, turbo-spin echo techniques [64]. First pass hypoenhancement and native T1 sequences have been particularly promising, and Vijayakumar et al [65] have demonstrated the utility of non-contrast T1w imaging in the acute identification of chronic lesions in a canine

model of ventricular scar. Non-contrast agent based imaging techniques are particularly attractive as they can be repeated multiple times [66].

Clinical studies have also been performed, but accuracy of acute lesion evaluation validation is compromised by the absence of a gold standard. Detailed assessment of CMR imaging performed at 24 hours, validated by imaging at three months, has corroborated that T2-weighted imaging tends to over-estimate chronic scar formation [67]. More recently, acute CMR imaging in a paediatric VT ablation cohort has shown a correlation with late clinical outcome [68].

CMR fused with X-ray

CMR can be used in cardiac catheterisation procedures either to directly guide the procedure or integrated with X-ray fluoroscopy. Integration with X-ray fluoroscopy can be done in 2 ways. One is to fuse the previously acquired 3D CMR image as an image overlay with fluoroscopic images, and the other is to use X-ray fluoroscopy to guide cardiac catheterisation, and then obtain physiological measurements such as intravascular flows and ventricular stroke volumes and function by means of CMR. Fusion of images has been utilised in cardiac catheter laboratories using pre-obtained CT, CMR or rotational angiographic images. This has been demonstrated to reduce the radiation exposure to the patient by means of pre-planning contrast angiographic projections from the 3D datasets, resulting in greater accuracy on the first attempt and fewer angiographic runs[69]. Additionally, it provides a roadmap for guiding cardiac catheter placement in complex anatomy without the need for multiples repeat contrast injections. There is an accepted registration error of up to 2mm and there are attempts to reduce this further by means of motion correction algorithms built into commercial and research systems. Most commercial systems

allow image overlay in one fluoroscopic plane, although biplane image overlay systems are being developed. The disadvantage of this approach is that once stiff wires and deployment sheaths are passed through the chambers and vessels of the heart, this can distort the anatomy compared to the original 3D dataset, resulting in a significant discrepancy in the image overlay (Figure 1). Combined X-ray and CMR can also be used in the hybrid CMR suite to define soft tissue changes post intervention, for example post stenting of aortic coarctation.

Figure 1 Images from a rotational angiogram overlayed onto x-ray fluoroscopy during percutaneous pulmonary valve implantation. In figure 1a, the image overlay appears good. During deployment of the valve, the use of a stiff wire distorts the anatomy of the right ventricular outflow tract and the previously acquired 3d angiogram is no longer in line with the fluoroscopic image.

Interventional cardiovascular magnetic resonance systems

In the design of an interventional CMR suite, it is important to retain the full capabilities of a state-of-the-art diagnostic scanner without encumbering the interventionist or creating a risk of high radiofrequency (RF). Open-magnet designs allow easier access to the patient, but are only available at low field strengths. The cylindrical horizontal bore systems offer higher field strengths and gradient slew rates, allowing higher-resolution imaging, shorter scan times, higher signal-to-noise ratio, reduced image distortion, and improved functionality with real-time imaging, all of which are essential for endovascular interventions [70]. However, the traditional cylindrical magnet design limits access to the patient, especially in small children and babies. Newer magnets with shorter bores and flared margins offer better patient access without compromising the advanced CMR features of diagnostic scanners.

Despite the inherent potential and promise of CMR-guided interventions and operations, the major obstacle is the lack of CMR-compatible catheters and devices. Therefore, the initial work in

interventional CMR exploited multi-modality imaging, such as X-ray and CMR (XMR) or XMR and ultrasound. Such hybrid units already in existence allow the use of separate modalities or a combination of them when needed, such as XMR systems, which combine X-ray and CMR by having both modalities in the same room, with a tabletop design that allows patients to be moved from one modality to the other in less than 1 minute (Figure 2)[71-74].

Figure 2 XMR room with the X-ray and MR equipment joined by a movable tabletop. The c-arm of the X-ray unit is seen in the foreground, ceiling-mounted MR monitor and controls are seen in the distance, and the 5-gauss area is demarcated by a change in the floor colouring from the MR to the X-ray end of the room.

Visualisation

Visualisation requirements include real-time acquisition and near real-time reconstruction, rapid sequence changes, interactive control and simultaneous visualization of a catheter or device and soft tissue. Improvements in the use of parallel imaging combined with improved processing power of computers to support post-processing software, have allowed the development of faster strategies for image data acquisition and reconstruction. This includes novel motion correction algorithms which allow for rapid and accurate free breathing acquisitions[75,76]. It is now possible to achieve frame rates of as high as 20 images/sec with the aid of new parallel imaging techniques while maintaining suitable spatial resolution for interventional applications[77-82].

Crucial to the success of interventional CMR is real-time tracking and visualization of catheters, guidewires, and devices in the CMR environment. Device localization under CMR is made possible by a variety of approaches that can be broadly classified as either electrically passive or electrically active[83].

Passive Catheter Tracking and Visualization

The passive tracking technique is commonly based on visualization of susceptibility artefacts or signal voids caused by the interventional device under CMR imaging. This is a well-studied technique and is clinically feasible[84-88] as it does not require any special hardware or software and therefore it can be performed on any commercial CMR system.

The ideal passive tracking catheter or guidewire must be made of a material that provides adequate physical properties such as torque and steerable and allows tracking without obscuring the underlying anatomy. Ferromagnetic materials cause large susceptibility artefacts and therefore are not generally suitable for CMR-guided procedures. Alloys, such as nitinol (nickel and titanium), have magnetic susceptibility close to that of tissue. Therefore, they are best suited for making guidewires and braided catheters but not necessarily CMR safe.

The polymeric materials used for making catheters typically have low magnetic susceptibility and therefore cannot be easily localized on CMR images[62]. Attempts generating susceptibility artefacts by locally impregnating the catheter wall with gadolinium-like compounds[88] or using gadolinium contrast agents in varying concentrations within catheter lumens[89] to create either a positive or negative signal on CMR imaging[90] have had limited success.

Metallic devices and guidewires produce susceptibility artefacts that aid visualization by way of the artefacts. Commercial guidewires can heat up during CMR because of standing wave formation along the conductive parts longer than a quarter wavelength at the resonant frequency, which

corresponds to approximately 12 cm in humans at 1.5T[91] where wires are inserted to at least that length and nearly always much further for cardiac catheterisation.

Guidewires with a fiberglass core and non-metallic guidewires made of resin microparticle compound covered by polytetrafluoroethylene have been used for MR-guided interventions in animals[92,93] and successful clinical trials with interventions in congenital heart disease but these have had been difficult to steer and proved to be fragile [94,95]. Consequently, a newer nitinol based guidewire with iron oxide markers along the length to impart visibility has been developed with good preclinical results[96].

Balloon angiographic catheters inflated with carbon dioxide, as is done conventionally with X-ray, creates a signal void in the CMR image enabling visualization of the tip (Figure 3).

Figure 3 Passive tracking. Inflated balloon angiographic Bermann catheter filled with 0.8 mL CO_2 from the inferior vena cava to the right pulmonary artery using solely magnetic resonance guidance. *Arrows* show the signal void of the catheter tip as it traverses the inferior vena cava, right atrium, tricuspid valve, and right ventricular outflow tract and enters the pulmonary artery.

This method has been used successfully to guide catheters in patients under CMR as form of 'negative contrast' imaging [14,97]. However, the length of the catheter is impossible to visualize because the signal void from the catheter length is masked by volume averaging and dephasing effects of thicker slices[98]. A similar approach is to inflate the balloon of the angiographic catheter with a 1% concentration of gadolinium contrast agent[16] and the balloon appears as a white ball due to the signal from the contrast-filled balloon as a form of "positive contrast" imaging.

The success of passive visualization also relies on dedicated scan techniques. A dynamic gradient echo sequence, such as SSFP, has been shown to be ideal for passive catheter tracking, especially when signal voids or susceptibility artefacts are used for visualization[97,99]. Cardiac catheterization under XRF guidance is usually performed at imaging speeds of 25 to 30 frames/sec. The frame rates available for CMR-guided interventions are not comparable because of the post-processing of CMR images and their subsequent display, allowing a maximum of 10 to 14 frames routinely. Positive contrast visualization is often used by means of using and 'on/off' saturation pulse combined with black blood imaging, where the interventional cardiologist visualizes either the soft tissue or catheter tip between rapidly changing image frames[16]. We have also introduced a partial saturation pulse using a real-time single shot acquisition with bssfp readout where each image is acquired immediately after a saturation pre-pulse with a reduced saturation angle to achieve partial saturation with a temporal resolution of ~7 images per second. The pSAT sequence offers real-time simultaneous high contrast visualization of the catheter balloon and blood (Figure 4). This technique provides excellent passive tracking capabilities during MR-guided catheterization in patients[100].

Figure 4 PSat sequence guidance of a catheter filled with gadolinium in the inferior vena cava of a patient with a cavopulmonary connection. The gadolinium filled tip appears bright white on this image.

The use of passive tracking requires significant input from a skilled CMR operator in order to manipulate the imaging plane to keep the device within slice. This is relatively easily achieved in narrow tubular structures lying within a single plane, such as the aorta, but is much more difficult when there is a greater degree of three-dimensional movement as is the case for an EP study or ablation within larger cardiac chambers. Thicker imaging slices (>10mm) improve the ability to

keep the device within plane, but CNR may be impaired to such a degree that the device may not be identifiable. There are also two further substantial limitations to passive tracking pertinent to MR-guided EP. The first is the difficulty in tracking more than one device at a time: EP frequently requires multiple diagnostic and ablation catheters, and the narrow MR imaging planes, in contrast to the projection view of fluoroscopy, limits the monitoring of more than one device at a time. The second limitation is the requirement to record location relative to cardiac structures. Automated image recognition techniques could theoretically be employed when the device tip is in-plane with sufficient CNR, enabling device localization to be referenced to pre-defined chambers, but such techniques have not been developed for clinical use.

Active Catheter Tracking and Visualization

The active catheter tracking and visualization method uses an electrical connection to the CMR scanner where the device is equipped with a coil or an antenna that functions in either receive-only mode or transmit/receive mode.

Active catheters that are used as receivers have a coil or an antenna that receives signal from tissue in its immediate vicinity[101]. These devices rely on the body coil to transmit into the patient. The signal received by these coils is used to pinpoint their position. There are two important types of active catheters: those based on small coils positioned, for example, at the end of a catheter, and those based on a loopless antenna that can run along a catheter or can be made into a guidewire[102-106].

A small resonant coil at the tip of a catheter can be identified by a series of three one-dimensional projections along each axis[101]. This can be done quickly (in three repetition times) and so could be repeated for very fast update of the catheter position, allowing real-time tracking of the catheter. The position of the catheter could then be projected over a previously acquired road map. Similar techniques have been combined with fast/real-time sequences, imaging the heart or vessels using surface coils, and the combined (interleaved) sequence has allowed visualization of two simultaneously acquired planes as well as visualization of the catheter or device positions in real time[107-110]. Active visualization has great potential because it allows the whole length of the catheter or guidewire to be visualized and the imaging plane to be adapted to the moving catheter automatically. These devices use intravascular coils as RF antennas, and the connection to the external circuits via a long wire in the strong magnetic field makes induction of an electrical current and heating possible.

There are technical challenges regarding RF safety in particular for long transmission lines, which must remain capable of conducting μV MR-receive signals. An approach based upon miniature transformers in the device has been proven to provide both the required tracking robustness and RF safety [111,112] and further work has resulted in dedicated EP catheters based on this approach [113,114]. Furthermore, multiple coils can be tracked simultaneously using the same tracking sequence, as it is limited only by the number of receivers.

SAFETY

Heating and Electrical Safety of Interventional Equipment

The potential heating of wires, devices, implants, and other instruments is an important factor in CMR development. Intravascular guidewires or device delivery systems with a metal core are unsafe in the CMR environment, with documented heating up to 74° C (165° F) of the tip[115-118]. In addition to the bioeffects of CMR and heating and electrical safety of interventional devices, a significant risk to interventional procedures is magnetic force and torque exerted by the magnetic field on metallic devices[119,120]. Interventional devices that are ferromagnetic will be subject to both deflection force (translational movement) and torque (rotational movement); therefore, they cannot be used for procedures within a CMR scanner. Conventional guidewires made of ferromagnetic materials, such as stainless steel, and catheters with metallic braiding, are inherently unsafe for use in the CMR environment. However, certain other metallic alloys, such as nitinol are CMR compatible and are not affected by the magnetic field in terms of deflection force and torque but can still be susceptible to heating and still be unsuitable for use in CMR procedures.

X-RAY AND CARDIOVASCULAR MAGNETIC RESONANCE GUIDANCE

X-Ray and Cardiovascular Magnetic Resonance Facility Design

The design and clinical practice framework for our XMR facility is outlined in a paper by White el al.[121]. The room design of a typical XMR facility is shown in Figure 2. The XMR suite is designed so that half of the room is outside the 5-gauss line of the magnet, permitting the use of traditional instruments and devices as well as echocardiography and RF ablation equipment when required. A movable tabletop allows patients to be moved easily and quickly between modalities.

The paramount consideration in the design, construction, and operation of an XMR facility is safety, and a comprehensive safety protocol must be drawn up to minimize possible hazards.

Traditionally, CMR scans are planned and conducted from the control room, away from the magnet and the patient. However, during CMR-guided cardiac catheterization, there is a need for real-time changes to the scanning plane and sequence parameters to follow catheter manipulation in the heart and great vessels. Also, the person carrying out the procedure needs to have a clear view of the CMR images while performing the cardiac catheter. Therefore, it is useful to have a fully functional set of ceiling-mounted, movable screens and scanner controls within the CMR scanner room that can be placed at either end of the bore of the scanner, in close proximity to the patient. Some units also have the facility for image overlay with semi-automated whole heart segmentation tools[122] and these are now commercially available (Interactive Front End, Siemens; RTHawk, HeartVista; Cleartrace, MRI Interventions; iSuite, Philips). These platforms have made it possible to manipulate through 3 orthogonal planes using an in-room foot pedal to guide live cardiac catheterisation in the MRI scanner.

The XMR suite also includes appropriate CMR-compatible anaesthetic equipment and monitoring equipment for invasive pressure monitoring via the catheter. All of the anaesthetic and monitoring tubing and lines are designed with extra length and are secured to the movable tabletop to ensure smooth patient transfer.

The electrocardiogram (ECG) and invasive pressure data are sent from the MR-compatible monitoring equipment via an optical network to a computer in the control room, where the cardiac

technician is stationed. The appropriate measurement and recording of the data is made in the usual way. The technician has access to monitors that show the appropriate X-ray or CMR images of the procedure. The person carrying out the procedure in the room can view the CMR images and any monitoring data (e.g., ECG, invasive pressure data) with the addition of commercially available MR conditional LCD monitors or projectors available for use in the MRI room for display. Blood samples taken during the procedure are labelled in the room and passed to the technician in the control room via a wave-guide.

Reliable and accurate ECG synchronization is essential for CMR and in particular CMR-guided cardiac catheterization. When catheters are manipulated in the heart, there is the potential to cause arrhythmias (tachyarrhythmia or heart block). It is therefore important to perform accurate monitoring of the cardiac rhythm at all times during XMR catheterization. Obtaining a reliable ECG in the magnet, particularly during some CMR sequences, can be difficult. Vector electrocardiogram (VCG) is a QRS detection algorithm that automatically adjusts to the actual electrical axis of the patient's heart and the specific multidimensional QRS waveform. In our experience, this greatly improves the reliability of R-wave detection to nearly 100%. A reliable R-wave, with the P- and T-waves that are also always clearly seen with VCG, allows detection of nearly all arrhythmias. There are now MR-conditional hemodynamic monitoring systems are available (Invivo, GE, Medrad) and are sufficient for basic monitoring, but there are still not commercial hemodynamic monitoring systems available specifically for use during MR guided cardiac catheterisation.

Another challenge of performing cardiac catheterization under CMR guidance is the noise generated during scanning. There is a headphone and microphone system in the room that reduces the noise, but allows staff to communicate with each other in both the scanner and control rooms. There are techniques using infra-red technology to allow full wireless coverage in the scanning and control rooms to allow use of multiple headsets (Opto-acoustics, Clear-com, Gaven).

Some CMR coils have X-ray-visible components and would need to be removed between CMR imaging and X-ray imaging of patients. It is therefore necessary to have specifically designed coils that are sufficiently radiotranslucent to be left in place during XRF without deterioration of image quality. We use these type of coils in our procedures so that patients do not have to be disturbed when moving from one imaging modality to the other[123].

The XMR suite has positive-pressure air handling and filtration appropriate for a catheterization laboratory. There is a scrub room that is also RF and X-ray shielded and can be accessed both from the XMR suite and control room.

Images of a standard MRI catheterisation in action are displayed in Figure 5.

Figure 5 X-ray and magnetic resonance intervention. 5a. Patient is placed on the magnetic resonance tabletop on the X-ray half of the room for sheath insertion. The MRI coils are demonstrated inset. 5b Image artefact from MRI coils on X-ray fluoroscopy. 5c. Patient is slid into the MRI scanner for MRI guided catheterisation. 5d. Image of foot pedals for in-room manipulation of the imaging planes by the primary operator.

Specific challenges for EP in the MR environment

The performance of EP procedures in the MR environment presents additional challenges over and above those encountered elsewhere.

Electrogram fidelity

Conventional electrophysiological procedures rely upon the detection of high quality surface and intracardiac electrograms, in order to detect accurately timings, changes and abnormalities of cardiac activation. However, the MR-environment, particularly time-variable gradient fields and magneto-hydrodynamic effects, act to corrupt the low-voltage signals.

Clinically, the surface ECG is currently limited to calculation from four surface adhesive electrodes (Expression, Invivo Medical, Gainesville, FL, USA), with marked distortion of many components of the ECG. Identification of the ST-segment and P-wave is often obscured, and many groups are working on improving the electrogram quality and enabling 12-lead ECG assessment [124]. A 12-lead ECG would be particularly useful for ventricular arrhythmia procedures and is a major hurdle to clinical implementation.

There are also challenges related to the detection and transmission of the intra-cardiac electrograms (IEGMs). As for a conventional EP laboratory, IEGMs must be high-pass and low-pass filtered, often with the addition of further notch filters to account for the frequency of mains electricity and other identified sources of noise. Despite filtering however, electrical noise levels remain high in the MR-environment and the IEGM voltage must be transmitted via a high resistivity, RF safe, transmission line. IEGM fidelity will need to improve significantly in order to enable detection of

low amplitude signals such as late diastolic potentials [125] but technical solutions are evolving rapidly [126].

Anaesthesia and monitoring

MR-guided EP procedures are currently longer than equivalent procedures using conventional guidance, and they are performed in a noisy and potentially claustrophobic environment. Therefore, published human studies have been performed under general anaesthesia or deep sedation [125-129]. The fundamentals of maintaining and monitoring anaesthesia in the MR-scanner room do not differ from those for non-EP procedures, but for longer procedures (up to five hours) particular attention is required in stabilizing body temperature and monitoring pressure areas.

A further consideration is the relatively high risk of arrhythmias in this patient group. There is currently no commercial MR-conditional defibrillator solution that has been released, although there is ongoing work to develop the capabilities [130]. Therefore, robust protocols and training must be in place for evacuation of the patient to a safe zone for medical resuscitation if required.

Early Experience in Humans

In our institution we had the first clinical experience of CMR and combined CMR and X-ray (XMR) guided cardiac catheterizations[14,34,97], which allowed for a significant reduction of overall X-ray dose. CMR/XMR catheterizations were initially employed and validated against standard cardiac catheterization for the assessment of pulmonary vascular resistance (PVR)[14,34]. This novel MR technique proved to be a more accurate method to quantify PVR in humans; it also offers reduced exposure to ionizing radiation[15,34].

In the past few years the indications have widened to include assessment of anatomy and function, cardiac output and hemodynamic measurements during pharmacological stress[17,35,37,39,131]. We have also described an initial clinical experience of CMR guided structural cardiac interventions using a CMR compatible guide wire[95]. CMR catheterisation has been employed successfully into routine clinical practice at several centres with experience of over 100 cases [16]. At our own unit, we have performed over 214 MRI catheterisations in the first 10 years of the programme[17] in a range of patient weights from 2.3kg to 108kg with a good safety profile. This includes the CMR guided interventions in man as described below. The majority of the assessments were for PVR evaluation. We found that PVR assessments in this way were a safe and accurate tool, which allowed for risk stratification of patients with congenital heart disease being considered for intervention [35].

Pharmacological stress studies with dobutamine are employed to increase the heart rate and simulate physiological heart rate responses to exercise to assess the circulation at rest and under 'stress'. These studies involved measurements of cardiac output and invasive pressures at baseline and are repeated with dobutamine infused at a rate of 10mcg/kg/min for 10 minutes or once a stable heart rate or blood pressure rise had been observed and repeated at 20mcg/kg/min. Thus far, these are employed in the assessment of patients pre-liver transplant [17,40] and in patients with a functionally single ventricle[39,41]. Our experience that titration in this manner has a very good safety profile. Isoprenaline stress studies have been used to assess for latent coarctation[43,132].

Interventional Structural/Congenital Cardiac Procedures

Animal models have shown immense potential of interventional CMR (Figure 6). The interventions that were shown to be feasible with passive and active catheter techniques include balloon angioplasty of arterial stenoses[133-138],stenting of vessels,[139-143] and atrial septal puncture/septostomy[144,145]. Device closure of atrial septal defects is another application that has been explored[146-149]. CMR-guided percutaneous pulmonary and aortic valve stent implantation have also been performed successfully (Fig. 44-11)[140,150]. More complex interventions, such as percutaneous coronary catheterization and intervention, have also been demonstrated in healthy animals using CMR[151-154] but limitations in spatial resolution are unlikely to result in coronary interventions being a key area for CMR guided interventions.

Figure 6 Schematic of the history of MRI catheterisation in humans and animals. Boxes marked in red relate to human studies. Boxes marked white relate to animal studies.

Further animal studies also offer potential interventions in congenital heart disease such as, percutaneous VSD closure[155] and successful transcatheter creation of bidirectional Glenn shunts in pigs [156]. The application of interventions has now been extended to humans [95,138]. This includes balloon dilation of aortic coarctation and pulmonary valvuloplasty in patients under CMR guidance alone. In our experience, the youngest patient where this has been achieved was 3.5 years[17,95].

Novel catheters and guidewires have made possible targeted intramyocardial injection of progenitor stem cells in myocardial infarction in animal models [109,157-159]. Using real-time CMR and direct apical access in porcine hearts, prosthetic aortic valves were implanted in the beating

heart[160]. This breakthrough application may allow CMR guidance of minimally invasive extra-anatomic bypass and beating-heart valve repair. MR guidance of intramyocardial gene therapy is another exciting field[161]. The ability of CMR to detect myocardial fibrosis and scar could also open up the utility for targeted myocardial biopsy with researchers working on developing appropriate biotomes[12]. This may well improvement the poor diagnostic yield of myocardial biopsy in the evaluation of cardiomyopathy[162].

MR-guided EP Procedures

Research in CMR-guided EP requires a broad team including physicists, engineers, radiologists, electrophysiologists and computer scientists. As such, work has been limited to relatively few centers worldwide. Pioneering studies by the group in Johns Hopkins established the benchmarks for the field in 2000 and highlighted the technical challenges that remained to be overcome [163]. Progress over the next decade was also made by teams in Boston (USA), Würzberg (Germany) and included the implementation of active tracking [59]and novel carbon catheters [164].

More recently, centers in London (UK), Utah (USA) and Leipzig (Germany) have advanced the field further towards mainstream clinical implementation. Early clinical work using passive tracking techniques [128,165] for atrial flutter ablation have advanced to active tracking techniques with a workflow resembling that of a conventional EP laboratory [125,126]. Over the next few years it is anticipated that CMR-guided EP technology (ablation catheters, digital amplifier stimulators, MR-conditional defibrillators) will be commercially available and that the technology will advance rapidly towards mainstream adoption for specific EP procedures. An example of CMR-guided EP platform used during clinical ablation of atrial flutter is given in Figure 7.

Figure 7 CMR-guided EP platform during clinical ablation of atrial flutter using active tracking (iSuite, Philips Research, Hamburg). All four panels are demonstrated simultaneously to the electrophysiology operator. The two left hand panels show orthogonal reconstructions of a b-SSFP 3D dataset (multiplanar reconstruction (MPR) 1 and 2). Location of prior ablation lesions are shown as red dots. Ablation catheter icon is red, and diagnostic/pacing catheter in green. The upper right hand panel is a single frame of a cine acquisition acquired a few seconds before, automatically oriented along the shaft of the ablation catheter, demonstrating the ablation catheter position. The lower right hand panel shows a close-up of the right atrial shell and the locations of the ablation lesions. Colour-coding is according to the timing of atrial activation on mapping whilst pacing from the coronary sinus, with earliest activation shown in red.

Future perspectives

There is a move for industry participation in the development of CMR compatible cardiac catheters and devices specifically designed for CMR-guided cardiac catheterization. This is particularly relevant in congenital heart disease, where complex anatomy requires wires and end-hole catheters with good steerabilty and torque to negotiate the bends of the relevant cardiac and vascular structures. Development needs to keep pace with the rigorous processes of regulatory approval involved in bringing devices and sequences from a prototype stage to clinical applications.

The cost associated with installing expensive XMR suites, does also limit the widespread application of interventional CMR but costs will eventually come down. Over time, there will need to be some verification in terms of the cost-effectiveness of these techniques and its role in improving patient outcomes. However, CMR guided catheterisation in children will continue to develop as a consequence of the continued strive for better anatomical and physiological data and avoidance of radiation.

Alternative approaches to RF safety

An alternative approach being pursued at the moment is to reduce the potential heating effects of radiofrequency (RF) from the scanner to allow use of standard metallic guidewires and catheters in the CMR environment. This is particularly relevant in CHD where there it would be advantageous to access the wide range of commercially available devices have been specially designed to accommodate the range of structural lesions. The application of parallel transmit technology allows the potential to improve visualisation of the catheter or wire in its entire length without inducing any dangerous heating. Using an 8-Channel prototype parallel transmit system and RF-efficient spiral gradient echo (GRE) imaging we have shown reduced heating of nitinol guidewires under CMR to a negligible level. This can then be combined with positive contrast imaging to improve visualization of the guidewire in vivo, with promising results, which may lead to the use of commercial nitinol guidewires safely and effectively for CMR-guided catheterizations.

There are now simulation methods of analyzing induced phase artefacts seen in low specific absorption rate characterization images, to determine induced current on an interventional device [166]. This induced current distribution can then be used to predict RF heating behaviour under application of any other imaging sequence without the need to induce potentially damaging heating in patients during testing.

Conclusion

CMR is already in use for diagnostic catheterization with proof of concept seen for interventional MRI and EP. There are significant advancements in scanning protocols, segmentation and

visualization/interaction tools which are making significant inroads on the historical barriers to progress due to issues related to hardware and software.

Acknowledgments

Some of the work described in this chapter was performed by a team of academic and clinical staff at the Evelina London Children's Hospital, London, United Kingdom and the Division of Imaging Sciences and Biomedical Engineering at King's College London. We wish to acknowledge Tobias Schaeffter, Kawal Rhode, Aphrodite Tzifa, Stephen Keevil, Marc O'Neill, Shakeel Qureshi, and Eric Rosenthal in the Departments of Imaging Sciences, Paediatric and Adult Cardiology.

References

1. Johnson JN, Hornik CP, Li JS, Benjamin DK, Yoshizumi TT, Reiman RE, Frush DP, Hill KD. Cumulative radiation exposure and cancer risk estimation in children with heart disease. *Circulation*. 2014;130:161–167.

2. Bashore TM, Bates ER, Berger PB, Clark DA, Cusma JT, Dehmer GJ, Kern MJ, Laskey WK, O'Laughlin MP, Oesterle S, Popma JJ, O'Rourke RA, Abrams J, Brodie BR, Douglas PS, Gregoratos G, Hlatky MA, Hochman JS, Kaul S, Tracy CM, Waters DD, Winters WL, American College of Cardiology. Task Force on Clinical Expert Consensus Documents. American College of Cardiology/Society for Cardiac Angiography and Interventions Clinical Expert Consensus Document on cardiac catheterization laboratory standards. A report of the American College of Cardiology Task Force on Clinical Expert Consensus Documents. 2001. p. 2170–2214.

3. McCullough PA, Wolyn R, Rocher LL, Levin RN, O'Neill WW. Acute renal failure after coronary intervention: incidence, risk factors, and relationship to mortality. *Am J Med*. 1997;103:368–375.

4. Venneri L, Rossi F, Botto N, Andreassi MG, Salcone N, Emad A, Lazzeri M, Gori C, Vano E, Picano E. Cancer risk from professional exposure in staff working in cardiac catheterization laboratory: insights from the National Research Council's Biological Effects of Ionizing Radiation VII Report. *American Heart Journal*. 2009;157:118–124.

5. Chambers CE, Fetterly KA, Holzer R, Lin P-JP, Blankenship JC, Balter S, Laskey

WK. Radiation safety program for the cardiac catheterization laboratory. *Catheter Cardiovasc Interv*. 2011;77:546–556.

6. Le Heron J. Guidelines on patient dose to promote the optimisation of protection for diagnostic medical exposures : documents of the NRPB v 10(1), 1999. *Radiation protection news and notes*. 1999;:17–18.

7. Little MP, De Vathaire F, Charles MW, Hawkins MM, Muirhead CR. Variations with time and age in the risks of solid cancer incidence after radiation exposure in childhood. *Stat Med*. 1998;17:1341–1355.

8. Modan B, Keinan L, Blumstein T, Sadetzki S. Cancer following cardiac catheterization in childhood. *Int J Epidemiol*. 2000;29:424–428.

9. Risk of ionizing radiation exposure to children: a subject review. American Academy of Pediatrics. Committee on Environmental Health. *Pediatrics*. 1998;101:717–719.

10. Jolesz FA, Blumenfeld SM. Interventional use of magnetic resonance imaging. *Magn Reson Q*. 1994;10:85–96.

11. Lufkin RB. Interventional MR imaging. *Radiology*. 1995;197:16–18.

12. Rogers T, Lederman RJ. Interventional CMR: Clinical Applications and Future Directions. *Curr Cardiol Rep*. 2015;17:31–9.

13. Rogers T, Ratnayaka K, Lederman RJ. MRI catheterization in cardiopulmonary disease. *Chest*. 2014;145:30–36.

14. Razavi R, Hill DLG, Keevil SF, Miquel ME, Muthurangu V, Hegde S, Rhode K, Barnett M, van Vaals J, Hawkes DJ, Baker E. Cardiac catheterisation guided by MRI in children and adults with congenital heart disease. *Lancet*. 2003;362:1877–1882.

15. Kuehne T, Yilmaz S, Schulze-Neick I, Wellnhofer E, Ewert P, Nagel E, Lange P. Magnetic resonance imaging guided catheterisation for assessment of pulmonary vascular resistance: in vivo validation and clinical application in patients with pulmonary hypertension. *Heart*. 2005;91:1064–1069.

16. Ratnayaka K, Faranesh AZ, Hansen MS, Stine AM, Halabi M, Barbash IM, Schenke WH, Wright VJ, Grant LP, Kellman P, Kocaturk O, Lederman RJ. Real-time MRI-guided right heart catheterization in adults using passive catheters. *European Heart Journal*. 2013;34:380–389.

17. Pushparajah K, Tzifa A, Razavi R. Cardiac MRI catheterization: a 10-year single institution experience and review. *Interventional Cardiology*. 2014;6:335–346.

18. Rogers T, Ratnayaka K, Karmarkar P, Campbell-Washburn AE, Schenke WH,

Mazal JR, Kocaturk O, Faranesh AZ, Lederman RJ. Real-time magnetic resonance imaging guidance improves the diagnostic yield of endomyocardial biopsy. *JACC Basic Transl Sci*. 2016;1:376–383.

19. Cigarroa RG, Lange RA, Hillis LD. Oximetric quantitation of intracardiac left-to-right shunting: limitations of the Qp/Qs ratio. *The American Journal of Cardiology*. 1989;64:246–247.

20. Dhingra VK. Lack of Agreement Between Thermodilution and Fick Cardiac Output in Critically Ill Patients*. *Chest*. 2002;122:990–997.

21. Hillis LD, Firth BG, Winniford MD. Variability of right-sided cardiac oxygen saturations in adults with and without left-to-right intracardiac shunting. *AJC*. 1986;58:129–132.

22. van den Berg E, Pacifico A, Lange RA, Wheelan KR, Winniford MD, Hillis LD. Measurement of cardiac output without right heart catheterization: reliability, advantages, and limitations of a left-sided indicator dilution technique. *Cathet Cardiovasc Diagn*. 1986;12:205–208.

23. Hillis LD, Firth BG, Winniford MD. Analysis of factors affecting the variability of Fick versus indicator dilution measurements of cardiac output. *AJC*. 1985;56:764–768.

24. Dehmer GJ, Firth BG, Hillis LD. Oxygen consumption in adult patients during cardiac catheterization. *Clinical Cardiology*. 1982;5:436–440.

25. Beerbaum P, Korperich H, Barth P, Esdorn H, Gieseke J, Meyer H. Noninvasive Quantification of Left-to-Right Shunt in Pediatric Patients : Phase-Contrast Cine Magnetic Resonance Imaging Compared With Invasive Oximetry. *Circulation*. 2001;103:2476–2482.

26. Beerbaum P, Korperich H, Gieseke J, Barth P, Peuster M, Meyer H. Rapid Left-to-Right Shunt Quantification in Children by Phase-Contrast Magnetic Resonance Imaging Combined With Sensitivity Encoding (SENSE). *Circulation*. 2003;108:1355–1361.

27. Beerbaum P, Korperich H, Gieseke J, Barth P, Peuster M, Meyer H. Blood Flow Quantification in Adults by Phase-Contrast MRI Combined with Sense - A Validation Study. *J Cardiovasc Magn Reson*. 2005;7:361–369.

28. Firmin DN, Nayler GL, Klipstein RH, Underwood SR, Rees RSO, Longmore DB. In Vivo Validation of MR Velocity Imaging. *Journal of Computer Assisted Tomography*. 1987;11:751–756.

29. Kilner PJ, Manzara CC, Mohiaddin RH, Pennell DJ, Sutton MG, Firmin DN, Underwood SR, Longmore DB. Magnetic resonance jet velocity mapping in mitral and aortic valve stenosis. *Circulation*. 1993;87:1239–1248.

30. Hundley WG, Li HF, Hillis LD, Meshack BM, Lange RA, Willard JE, Landau C, Peshock RM. Quantitation of cardiac output with velocity-encoded, phase-difference magnetic resonance imaging. *The American Journal of Cardiology*. 1995;75:1250–1255.

31. Hundley WG, Li HF, Lange RA, Pfeifer DP, Meshack BM, Willard JE, Landau C, Willett D, Hillis LD, Peshock RM. Assessment of Left-to-Right Intracardiac Shunting by Velocity-Encoded, Phase-Difference Magnetic Resonance Imaging A Comparison With Oximetric and Indicator Dilution Techniques. *Circulation*. 1995;91:2955–2960.

32. Mousseaux E, Tasu JP, Jolivet O, Simonneau G, Bittoun J, Gaux J-C. Pulmonary Arterial Resistance: Noninvasive Measurement with Indexes of Pulmonary Flow Estimated at Velocity-encoded MR Imaging—Preliminary Experience1. *Radiology*. 1999;212:896–902.

33. Kondo C, Caputo GR, Masui T, Foster E, O'Sullivan M, Stulbarg MS, Golden J, Catterjee K, Higgins CB. Pulmonary hypertension: pulmonary flow quantification and flow profile analysis with velocity-encoded cine MR imaging. *Radiology*. 1992;183:751–758.

34. Muthurangu V, Taylor A, Andriantsimiavona R, Hegde S, Miquel ME, Tulloh R, Baker E, Hill DLG, Razavi RS. Novel method of quantifying pulmonary vascular resistance by use of simultaneous invasive pressure monitoring and phase-contrast magnetic resonance flow. *Circulation*. 2004;110:826–834.

35. Pushparajah K, Tzifa A, Bell A, Wong JK, Hussain T, Valverde I, Bellsham-Revell HR, Greil G, Simpson JM, Schaeffter T, Md RR. Cardiovascular Magnetic Resonance catheterization derived pulmonary vascular resistance and medium-term outcomes in congenital heart disease. *J Cardiovasc Magn Reson*. 2015;17:28.

36. Muthurangu V, Atkinson D, Sermesant M, Miquel ME, Hegde S, Johnson R, Andriantsimiavona R, Taylor AM, Baker E, Tulloh R, Hill D, Razavi RS. Measurement of total pulmonary arterial compliance using invasive pressure monitoring and MR flow quantification during MR-guided cardiac catheterization. *Am J Physiol Heart Circ Physiol*. 2005;289:H1301–6.

37. Kuehne T. Magnetic Resonance Imaging Analysis of Right Ventricular Pressure-Volume Loops: In Vivo Validation and Clinical Application in Patients With Pulmonary Hypertension. *Circulation*. 2004;110:2010–2016.

38. Schmitt B, Steendijk P, Lunze K, Ovroutski S, Falkenberg J, Rahmanzadeh P, Maarouf N, Ewert P, Berger F, Kuehne T. Integrated assessment of diastolic and systolic ventricular function using diagnostic cardiac magnetic resonance catheterization: validation in pigs and application in a clinical pilot study. *JACC: Cardiovascular Imaging*. 2009;2:1271–1281.

39. Schmitt B, Steendijk P, Ovroutski S, Lunze K, Rahmanzadeh P, Maarouf N, Ewert

P, Berger F, Kuehne T. Pulmonary Vascular Resistance, Collateral Flow, and Ventricular Function in Patients With a Fontan Circulation at Rest and During Dobutamine Stress. *Circulation: Cardiovascular Imaging*. 2010;3:623–631.

40. Razavi RS, Baker A, Qureshi SA, Rosenthal E, Marsh MJ, Leech SC, Rela M, Mieli-Vergani G. Hemodynamic response to continuous infusion of dobutamine in Alagille's syndrome. *Transplantation*. 2001;72:823.

41. Pushparajah K, Wong JK, Bellsham-Revell HR, Hussain T, Valverde I, Bell A, Tzifa A, Greil G, Simpson JM, Kutty S, Razavi R. Magnetic resonance imaging catheter stress haemodynamics post-Fontan in hypoplastic left heart syndrome. *Eur Heart J Cardiovasc Imaging*. 2016;17:644–651.

42. Wong J, Pushparajah K, de Vecchi A. Myocardial contractile response to dobutamine in hypoplastic left heart syndrome post-Fontan. *Journal of …*. 2014;

43. Valverde I, Staicu C, Grotenhuis H, Marzo A, Rhode K, Shi Y, Brown AG, Tzifa A, Hussain T, Greil G, Lawford P, Razavi R, Hose R, Beerbaum P. Predicting hemodynamics in native and residual coarctation: preliminary results of a Rigid-Wall Computational-Fluid-Dynamics model (RW-CFD) validated against clinically invasive pressure measures at rest and during pharmacological stress. *J Cardiovasc Magn Reson*. 2011;13:P49.

44. Wong J, Pushparajah K, de Vecchi A, Ruijsink B, Greil GF, Hussain T, Razavi R. Pressure-volume loop-derived cardiac indices during dobutamine stress: a step towards understanding limitations in cardiac output in children with hypoplastic left heart syndrome. *International Journal of Cardiology*. 2017;230:439–446.

45. Nazarian S, Bluemke DA, Lardo AC, Zviman MM, Watkins SP, Dickfeld TL, Meininger GR, Roguin A, Calkins H, Tomaselli GF, Weiss RG, Berger RD, Lima JAC, Halperin HR. Magnetic resonance assessment of the substrate for inducible ventricular tachycardia in nonischemic cardiomyopathy. *Circulation*. 2005;112:2821–2825.

46. Ashikaga H, Arevalo H, Vadakkumpadan F, Blake RC, Bayer JD, Nazarian S, Muz Zviman M, Tandri H, Berger RD, Calkins H, Herzka DA, Trayanova NA, Halperin HR. Feasibility of image-based simulation to estimate ablation target in human ventricular arrhythmia. *Heart Rhythm*. 2013;10:1109–1116.

47. Ashikaga H, Sasano T, Dong J, Zviman MM, Evers R, Hopenfeld B, Castro V, Helm RH, Dickfeld T, Nazarian S, Donahue JK, Berger RD, Calkins H, Abraham MR, Marbán E, Lardo AC, McVeigh ER, Halperin HR. Magnetic resonance-based anatomical analysis of scar-related ventricular tachycardia: implications for catheter ablation. *Circ Res*. 2007;101:939–947.

48. Marrouche NF, Wilber D, Hindricks G, JAÏS P, Akoum N, Marchlinski F, Kholmovski E, Burgon N, Hu N, Mont L, Deneke T, Duytschaever M, Neumann T, Mansour M, Mahnkopf C, Herweg B, Daoud E, Wissner E, Bansmann P,

Brachmann J. Association of atrial tissue fibrosis identified by delayed enhancement MRI and atrial fibrillation catheter ablation: the DECAAF study. *JAMA*. 2014;311:498–506.

49. Carbucicchio C, Ahmad Raja N, Di Biase L, Volpe V, Russo Dello A, Trivedi C, Bartoletti S, Zucchetti M, Casella M, Russo E, Santangeli P, Moltrasio M, Tundo F, Fassini G, Natale A, Tondo C. High-density substrate-guided ventricular tachycardia ablation: role of activation mapping in an attempt to improve procedural effectiveness. *Heart Rhythm*. 2013;10:1850–1858.

50. Pop M, Ghugre NR, Ramanan V, Morikawa L, Stanisz G, Dick AJ, Wright GA. Quantification of fibrosis in infarcted swine hearts by ex vivolate gadolinium-enhancement and diffusion-weighted MRI methods. *Phys Med Biol*. 2013;58:5009–5028.

51. Perez-David E, Arenal Á, Rubio-Guivernau JL, del Castillo R, Atea L, Arbelo E, Caballero E, Celorrio V, Datino T, Gonzalez-Torrecilla E, Atienza F, Ledesma-Carbayo MJ, Bermejo J, Medina A, Fernandez-Aviles F. Noninvasive identification of ventricular tachycardia-related conducting channels using contrast-enhanced magnetic resonance imaging in patients with chronic myocardial infarction: comparison of signal intensity scar mapping and endocardial voltage mapping. *Journal of the American College of Cardiology*. 2011;57:184–194.

52. Andreu D, Berruezo A, Ortiz-Pérez JT, Silva E, Mont L, Borràs R, de Caralt TM, Perea RJ, Fernández-Armenta J, Zeljko H, Brugada J. Integration of 3D electroanatomic maps and magnetic resonance scar characterization into the navigation system to guide ventricular tachycardia ablation. *Circ Arrhythm Electrophysiol*. 2011;4:674–683.

53. COCHET H, KOMATSU Y, SACHER F, JADIDI AS, SCHERR D, RIFFAUD M, DERVAL N, SHAH A, ROTEN L, PASCALE P, RELAN J, Sermesant M, Ayache N, MONTAUDON M, LAURENT F, HOCINI M, HAÏSSAGUERRE M, JAÏS P. Integration of merged delayed-enhanced magnetic resonance imaging and multidetector computed tomography for the guidance of ventricular tachycardia ablation: a pilot study. *J Cardiovasc Electrophysiol*. 2013;24:419–426.

54. Bisbal F, Guiu E, Cabanas-Grandío P, Berruezo A, Prat-Gonzalez S, Vidal B, Garrido C, Andreu D, Fernández-Armenta J, Tolosana JM, Arbelo E, de Caralt TM, Perea RJ, Brugada J, Mont L. CMR-guided approach to localize and ablate gaps in repeat AF ablation procedure. *JACC: Cardiovascular Imaging*. 2014;7:653–663.

55. Reddy VY, Malchano ZJ, Holmvang G, Schmidt EJ, d'Avila A, Houghtaling C, Chan RC, Ruskin JN. Integration of cardiac magnetic resonance imaging with three-dimensional electroanatomic mapping to guide left ventricular catheter manipulation: feasibility in a porcine model of healed myocardial infarction. *JAC*. 2004;44:2202–2213.

56. Fernandez-Armenta J, Berruezo A, Andreu D, Camara O, Silva E, Serra L, Barbarito

V, Carotenutto L, Evertz R, Ortiz-Perez JT, De Caralt TM, Perea RJ, Sitges M, Mont L, Frangi A, Brugada J. Three-Dimensional Architecture of Scar and Conducting Channels Based on High Resolution ce-CMR: Insights for Ventricular Tachycardia Ablation. *Circ Arrhythm Electrophysiol*. 2013;6:528–537.

57. Ranjan R, Kholmovski EG, Blauer J, Vijayakumar S, Volland NA, Salama ME, Parker DL, MacLeod R, Marrouche NF. Identification and Acute Targeting of Gaps in Atrial Ablation Lesion Sets Using a Real-Time Magnetic Resonance Imaging System. *Circ Arrhythm Electrophysiol*. 2012;5:1130–1135.

58. Steiner P, Botnar R, Goldberg SN. Monitoring of radio frequency tissue ablation in an interventional magnetic resonance environment: preliminary ex vivo and in vivo results. *Invest Radiol*. 1997;32:671–678.

59. Schmidt EJ, Mallozzi RP, Thiagalingam A, Holmvang G, d'Avila A, Guhde R, Darrow R, Slavin GS, Fung MM, Dando J, Foley L, Dumoulin CL, Reddy VY. Electroanatomic mapping and radiofrequency ablation of porcine left atria and atrioventricular nodes using magnetic resonance catheter tracking. *Circ Arrhythm Electrophysiol*. 2009;2:695–704.

60. Vergara GR, Vijayakumar S, Kholmovski EG, Blauer JJE, Guttman MA, Gloschat C, Payne G, Vij K, Akoum NW, Daccarett M, McGann CJ, Macleod RS, Marrouche NF. Real-time magnetic resonance imaging-guided radiofrequency atrial ablation and visualization of lesion formation at 3 Tesla. *Heart Rhythm*. 2011;8:295–303.

61. Toupin S, Bour P, Lepetit-Coiffé M, Ozenne V, Denis de Senneville B, Schneider R, Vaussy A, Chaumeil A, COCHET H, SACHER F, JAÏS P, Quesson B. Feasibility of real-time MR thermal dose mapping for predicting radiofrequency ablation outcome in the myocardium in vivo. *J Cardiovasc Magn Reson*. 2017;19:14.

62. Lardo AC. Real-time magnetic resonance imaging: diagnostic and interventional applications. *Pediatr Cardiol*. 2000;21:80–98.

63. Dickfeld T, Kato R, Zviman M, Nazarian S, Dong J, Ashikaga H, Lardo AC, Berger RD, Calkins H, Halperin H. Characterization of acute and subacute radiofrequency ablation lesions with nonenhanced magnetic resonance imaging. *Heart Rhythm*. 2007;4:208–214.

64. Nordbeck P, Hiller K-H, Fidler F, Warmuth M, Burkard N, Nahrendorf M, Jakob PM, Quick HH, Ertl G, Bauer WR, Ritter O. Feasibility of contrast-enhanced and nonenhanced MRI for intraprocedural and postprocedural lesion visualization in interventional electrophysiology: animal studies and early delineation of isthmus ablation lesions in patients with typical atrial flutter. *Circulation: Cardiovascular Imaging*. 2011;4:282–294.

65. Vijayakumar S, Ranjan R, Hong K, Kim D, Marrouche NF, Kholmovski EG. Assessment of cardiac RF ablation lesions by DCE-MRI. *J Cardiovasc Magn Reson*. 2014;16:P155.

66. Celik H, Ramanan V, Barry J, Ghate S, Leber V, Oduneye S, Gu Y, Jamali M, Ghugre N, Stainsby JA, Shurrab M, Crystal E, Wright GA. Intrinsic contrast for characterization of acute radiofrequency ablation lesions. *Circ Arrhythm Electrophysiol*. 2014;7:718–727.

67. Arujuna A, Karim R, Caulfield D, Knowles B, Rhode K, Schaeffter T, Kato B, Rinaldi CA, Cooklin M, Razavi R, O'Neill MD, Gill J. Acute pulmonary vein isolation is achieved by a combination of reversible and irreversible atrial injury after catheter ablation: evidence from magnetic resonance imaging. *Circ Arrhythm Electrophysiol*. 2012;5:691–700.

68. Grant EK, BERUL CI, CROSS RR, MOAK JP, HAMANN KS, SUMIHARA K, CRONIN I, O'BRIEN KJ, Ratnayaka K, Hansen MS, Kellman P, Olivieri LJ. Acute Cardiac MRI Assessment of Radiofrequency Ablation Lesions for Pediatric Ventricular Arrhythmia: Feasibility and Clinical Correlation. *J Cardiovasc Electrophysiol*. 2017;28:517–522.

69. Abu Hazeem AA, Dori Y, Whitehead KK, Harris MA, Fogel MA, Gillespie MJ, Rome JJ, Glatz AC. X-ray magnetic resonance fusion modality may reduce radiation exposure and contrast dose in diagnostic cardiac catheterization of congenital heart disease. *Catheter Cardiovasc Interv*. 2014;84:795–800.

70. Elgort DR, Duerk JL. A Review of Technical Advances in Interventional Magnetic Resonance Imaging1. *Academic Radiology*. 2005;12:1089–1099.

71. Fahrig R, Butts K, Rowlands JA, Saunders R, Stanton J, Stevens GM, Daniel BL, Wen Z, Ergun DL, Pelc NJ. A truly hybrid interventional MR/X-ray system: feasibility demonstration. *J Magn Reson Imaging*. 2001;13:294–300.

72. Fahrig R, Butts K, Wen Z, Saunders R, Kee ST, Sze DY, Daniel BL, Laerum F, Pelc NJ. Truly Hybrid Interventional MR/X-Ray System. *Academic Radiology*. 2001;8:1200–1207.

73. Adam G, Neuerburg J, Bücker A, Glowinski A, Vorwerk D, Stargardt A, Van Vaals JJ, Günther RW. Interventional magnetic resonance. Initial clinical experience with a 1.5-tesla magnetic resonance system combined with c-arm fluoroscopy. *Invest Radiol*. 1997;32:191–197.

74. Rhode KS, Hill DLG, Edwards PJ, Hipwell J, Rueckert D, Sanchez-Ortiz G, Hegde S, Rahunathan V, Razavi R. Registration and tracking to integrate X-ray and MR images in an XMR facility. *IEEE Trans Med Imaging*. 2003;22:1369–1378.

75. Steeden JA, Atkinson D, Taylor AM, Muthurangu V. Assessing vascular response to exercise using a combination of real-time spiral phase contrast MR and noninvasive blood pressure measurements. *Journal of Magnetic Resonance Imaging*. 2010;31:997–1003.

76. Xue H, Kellman P, Larocca G, Arai AE, Hansen MS. High spatial and temporal

resolution retrospective cine cardiovascular magnetic resonance from shortened free breathing real-time acquisitions. *J Cardiovasc Magn Reson*. 2013;15:102.

77. Bücker A, Neuerburg JM, Adam GB, Glowinski A, Schaeffter T, Rasche V, van Vaals JJ, Günther RW. Real-time MR Guidance for Inferior Vena Cava Filter Placement in an Animal Model. *Journal of Vascular and Interventional Radiology*. 2001;12:753–756.

78. Pruessmann KP, Weiger M, Scheidegger MB, Boesiger P. SENSE: Sensitivity encoding for fast MRI. *Magn Reson Med*. 1999;42:952–962.

79. Pruessmann KP, Weiger M, Boesiger P. Sensitivity Encoded Cardiac MRI. *J Cardiovasc Magn Reson*. 2001;3:1–9.

80. McVeigh ER, Guttman MA, Kellman P, Raval AN, Lederman RJ. Real-time, Interactive MRI for Cardiovascular Interventions1. *Academic Radiology*. 2005;12:1121–1127.

81. Yutzy SR, Duerk JL. Pulse sequences and system interfaces for interventional and real-time MRI. *J Magn Reson Imaging*. 2008;27:267–275.

82. Uecker M, Zhang S, Voit D, Karaus A, Merboldt K-D, Frahm J. Real-time MRI at a resolution of 20 ms. *NMR Biomed*. 2010;23:986–994.

83. Duerk J. A brief review of hardware for catheter tracking in magnetic resonance imaging. *Magnetic Resonance Materials in Biology, Physics, and Medicine*. 2002;13:199–208.

84. RUBIN DL, RATNER AV, YOUNG SW. Magnetic Susceptibility Effects and Their Application in the Development of New Ferromagnetic Catheters for Magnetic Resonance Imaging. *Invest Radiol*. 1990;25:1325–1332.

85. Bakker CJ, Hoogeveen RM, Weber J, van Vaals JJ, Viergever MA, Mali WP. Visualization of dedicated catheters using fast scanning techniques with potential for MR-guided vascular interventions. *Magn Reson Med*. 1996;36:816–820.

86. Bakker CJ, Smits HF, Bos C, van der Weide R, Zuiderveld KJ, van Vaals JJ, Hurtak WF, Viergever MA, Mali WP. MR-guided balloon angioplasty: In vitro demonstration of the potential of MRI for guiding, monitoring, and evaluating endovascular interventions. *J Magn Reson Imaging*. 1998;8:245–250.

87. Bakker CJG, Bos C, Weinmann HJ. Passive tracking of catheters and guidewires by contrast-enhanced MR fluoroscopy. *Magn Reson Med*. 2001;45:17–23.

88. Bakker CJ, Hoogeveen RM, Hurtak WF, Van Vaals JJ, Viergever MA, Mali WP. MR-guided endovascular interventions: susceptibility-based catheter and near-real-time imaging technique. *Radiology*. 1997;202:273–276.

89. Omary RA, Unal O, Koscielski DS, Frayne R, Korosec FR, Mistretta CA, Strother CM, Grist TM. Real-Time MR Imaging-guided Passive Catheter Tracking with Use of Gadolinium-filled Catheters. *Journal of Vascular and Interventional Radiology*. 2000;11:1079–1085.

90. Unal O, Li J, Cheng W, Yu H, Strother CM. MR-visible coatings for endovascular device visualization. *J Magn Reson Imaging*. 2006;23:763–769.

91. Yeung CJ, Susil RC, Atalar E. RF safety of wires in interventional MRI: using a safety index. *Magn Reson Med*. 2002;47:187–193.

92. Mekle R, Hofmann E, Scheffler K, Bilecen D. A polymer-based MR-compatible guidewire: A study to explore new prospects for interventional peripheral magnetic resonance angiography (ipMRA). *J Magn Reson Imaging*. 2006;23:145–155.

93. Buecker A, Spuentrup E, Schmitz-Rode T, Kinzel S, Pfeffer J, Hohl C, van Vaals JJ, Günther RW. Use of a nonmetallic guide wire for magnetic resonance-guided coronary artery catheterization. *Invest Radiol*. 2004;39:656–660.

94. Krueger S, Schmitz S, Weiss S, Wirtz D, Linssen M, Schade H, Kraemer N, Spuentrup E, Krombach G, Buecker A. An MR guidewire based on micropultruded fiber-reinforced material. *Magn Reson Med*. 2008;60:1190–1196.

95. Tzifa A, Krombach GA, Krämer N, Krüger S, Schütte A, Walter von M, Schaeffter T, Qureshi S, Krasemann T, Rosenthal E, Schwartz CA, Varma G, Buhl A, Kohlmeier A, Bücker A, Günther RW, Razavi R. Magnetic resonance-guided cardiac interventions using magnetic resonance-compatible devices: a preclinical study and first-in-man congenital interventions. *Circ Cardiovasc Interv*. 2010;3:585–592.

96. Basar B, Rogers T, Ratnayaka K, Campbell-Washburn AE, Mazal JR, Schenke WH, Sonmez M, Faranesh AZ, Lederman RJ, Kocaturk O. Segmented nitinol guidewires with stiffness-matched connectors for cardiovascular magnetic resonance catheterization: preserved mechanical performance and freedom from heating. *J Cardiovasc Magn Reson*. 2015;17:105.

97. Miquel ME, Hegde S, Muthurangu V, Corcoran BJ, Keevil SF, Hill DLG, Razavi RS. Visualization and tracking of an inflatable balloon catheter using SSFP in a flow phantom and in the heart and great vessels of patients. *Magn Reson Med*. 2004;51:988–995.

98. Zimmermann-Paul GG, Ladd ME, Pfammatter T, Hilfiker PR, Quick HH, Debatin JF. MR versus fluoroscopic guidance of a catheter/guidewire system: In vitro comparison of steerability. *J Magn Reson Imaging*. 1998;8:1177–1181.

99. Martin AJ, Weber OM, Saeed M, Roberts TPL. Steady-state imaging for visualization of endovascular interventions. *Magn Reson Med*. 2003;50:434–438.

100. Velasco Forte MN, Pushparajah K, Schaeffter T, Valverde Perez I, Rhode K, Ruijsink B, Alhrishy M, Byrne N, Chiribiri A, Ismail T, Hussain T, Razavi R, Roujol S. Improved passive catheter tracking with positive contrast for CMR-guided cardiac catheterization using partial saturation (pSAT). *J Cardiovasc Magn Reson*. 2017;19:60.

101. Dumoulin CL, Souza SP, Darrow RD. Real-time position monitoring of invasive devices using magnetic resonance. *Magn Reson Med*. 1993;29:411–415.

102. Ladd ME, Zimmermann GG, McKinnon GC, Schulthess von GK, Dumoulin CL, Darrow RD, Hofmann E, Debatin JF. Visualization of vascular guidewires using MR tracking. *J Magn Reson Imaging*. 1998;8:251–253.

103. Ladd ME, Zimmermann GG, Quick HH, Debatin JF, Boesiger P, Schulthess von GK, McKinnon GC. Active MR visualization of a vascular guidewire in vivo. *J Magn Reson Imaging*. 1998;8:220–225.

104. Ladd ME, Quick HH. Reduction of resonant RF heating in intravascular catheters using coaxial chokes. *Magn Reson Med*. 2000;43:615–619.

105. Zhang Q, Wendt M, Aschoff AJ, Zheng L, Lewin JS, Duerk JL. Active MR guidance of interventional devices with target- navigation. *Magn Reson Med*. 2000;44:56–65.

106. Hillenbrand CM, Elgort DR, Wong EY, Reykowski A, Wacker FK, Lewin JS, Duerk JL. Active device tracking and high-resolution intravascular MRI using a novel catheter-based, opposed-solenoid phased array coil. *Magn Reson Med*. 2004;51:668–675.

107. Guttman MA, Lederman RJ, Sorger JM, McVeigh ER. Real-Time Volume Rendered MRI for Interventional Guidance. *J Cardiovasc Magn Reson*. 2002;4:431–442.

108. Lederman RJ. Cardiovascular interventional magnetic resonance imaging. *Circulation*. 2005;112:3009–3017.

109. Lederman RJ, Guttman MA, Peters DC, Thompson RB, Sorger JM, Dick AJ, Raman VK, McVeigh ER. Catheter-based endomyocardial injection with real-time magnetic resonance imaging. *Circulation*. 2002;105:1282–1284.

110. Bell JA, Saikus CE, Ratnayaka K, Wu V, Sonmez M, Faranesh AZ, Colyer JH, Lederman RJ, Kocaturk O. A deflectable guiding catheter for real-time MRI-guided interventions. *J Magn Reson Imaging*. 2011;35:908–915.

111. Weiss S, Vernickel P, Schaeffter T, Schulz V, Gleich B. Transmission line for improved RF safety of interventional devices. *Magn Reson Med*. 2005;54:182–189.

112. Vernickel P, Schulz V, Weiss S, Gleich B. A safe transmission line for MRI. *IEEE*

Trans Biomed Eng. 2005;52:1094–1102.

113. Krueger S, Lips O, David B, Wirtz D, Weiss S, Pedersen SF, Caulfield D, Bostock J, Razavi R, Schaeffter T. Towards MR-guided EP interventions using an RF-safe approach. *J Cardiovasc Magn Reson*. 2009;11:O84.

114. Weiss S, Wirtz D, David B, Krueger S, Lips O, Caulfield D, Pedersen SF, Bostock J, Razavi R, Schaeffter T. In vivo evaluation and proof of radiofrequency safety of a novel diagnostic MR-electrophysiology catheter. *Magn Reson Med*. 2011;65:770–777.

115. Konings MK, Bartels LW, Smits HF, Bakker CJ. Heating around intravascular guidewires by resonating RF waves. *J Magn Reson Imaging*. 2000;12:79–85.

116. Liu C-Y, Farahani K, Lu DSK, Duckwiler G, Oppelt A. Safety of MRI-guided endovascular guidewire applications. *J Magn Reson Imaging*. 2000;12:75–78.

117. Shellock FG, Shellock VJ. Cardiovascular catheters and accessories: ex vivo testing of ferromagnetism, heating, and artifacts associated with MRI. *J Magn Reson Imaging*. 1998;8:1338–1342.

118. Nitz WR, Oppelt A, Renz W, Manke C, Lenhart M, Link J. On the heating of linear conductive structures as guide wires and catheters in interventional MRI. *J Magn Reson Imaging*. 2001;13:105–114.

119. Luechinger R, Duru F, Scheidegger MB, Boesiger P, Candinas R. Force and torque effects of a 1.5-Tesla MRI scanner on cardiac pacemakers and ICDs. *Pacing Clin Electrophysiol*. 2001;24:199–205.

120. Buecker A, Spuentrup E, Grabitz R, Freudenthal F, Schaeffter T, Van Vaals JJ, Günther W. Real-time-MR guidance for placement of a self-made fully MR-compatible atrial septal occluder: in vitro test. *Rofo*. 2002;174:283–285.

121. White MJ, Thornton JS, Hawkes DJ, Hill DLG, Kitchen N, Mancini L, McEvoy AW, Razavi R, Wilson S, Yousry T, Keevil SF. Design, Operation, and Safety of Single- Room Interventional MRI Suites: Practical Experience From Two Centers. *Journal of Magnetic Resonance Imaging*. 2015;41:34–43.

122. Peters J, Ecabert O, Meyer C, Schramm H, Kneser R, Groth A, Weese J. Automatic whole heart segmentation in static magnetic resonance image volumes. *Med Image Comput Comput Assist Interv*. 2007;10:402–410.

123. Rieke V, Ganguly A, Daniel BL, Scott G, Pauly JM, Fahrig R, Pelc NJ, Butts K. X-ray compatible radiofrequency coil for magnetic resonance imaging. *Magn Reson Med*. 2005;53:1409–1414.

124. Schmidt EJ, Dumoulin CL, Danik SA. Image-Guided Cardiac Electrophysiology Procedures Focusing on MRI Guidance. In: Intraoperative Imaging and Image-

Guided Therapy. New York, NY: Springer New York; 2013. p. 701–724.

125. Hilbert S, Sommer P, Gutberlet M, Gaspar T, Foldyna B, Piorkowski C, Weiss S, Lloyd T, Schnackenburg B, Krueger S, Fleiter C, Paetsch I, Jahnke C, Hindricks G, Grothoff M. Real-time magnetic resonance-guided ablation of typical right atrial flutter using a combination of active catheter tracking and passive catheter visualization in man: initial results from a consecutive patient series. *Europace*. 2015;18:572–577.

126. Chubb H, Harrison JL, Weiss S, Krueger S, Koken P, Bloch LØ, Kim WY, Stenzel GS, Wedan SR, Weisz JL, Gill J, Schaeffter T, O'Neill MD, Razavi RS. Development, Preclinical Validation, and Clinical Translation of a Cardiac Magnetic Resonance - Electrophysiology System With Active Catheter Tracking for Ablation of Cardiac Arrhythmia. *JACC: Clinical Electrophysiology*. 2017;3:89–103.

127. Chubb H, Harrison J, Williams SE, Weiss S, Rhode K, Krueger S, ONeill M, Schaeffter T, Razavi R. First in man: real-time magnetic resonance-guided ablation of typical right atrial flutter using active catheter tracking. *Europace*. 2014;16:iii23–iii23.

128. Grothoff M, Piorkowski C, Gaspar T, Hilbert S, Sommer P, Weiss S, Krüger S, Lloyd T, Schnackenburg B, Hindircks G, Gutberlet M. Comprehensive MRI-guided intracardiac electrophysiological interventions in swine using a combination of active tracking and passive real-time catheter imaging. *J Cardiovasc Magn Reson*. 2014;16:1.

129. Nazarian S, Kolandaivelu A, Zviman MM, Meininger GR, Kato R, Susil RC, Roguin A, Dickfeld TL, Ashikaga H, Calkins H, Berger RD, Bluemke DA, Lardo AC, Halperin HR. Feasibility of Real-Time Magnetic Resonance Imaging for Catheter Guidance in Electrophysiology Studies. *Circulation*. 2008;118:223–229.

130. Schmidt EJ, Watkins RD, Zviman MM, Guttman MA, Wang W, Halperin HA. A Magnetic Resonance Imaging-Conditional External Cardiac Defibrillator for Resuscitation Within the Magnetic Resonance Imaging Scanner Bore. *Circulation: Cardiovascular Imaging*. 2016;9:e005091.

131. Tzifa A, Schaeffter T, Razavi R. MR imaging-guided cardiovascular interventions in young children. *Magn Reson Imaging Clin N Am*. 2012;20:117–128.

132. Sotelo JA, Valverde I, Beerbaum PB, Greil GF, Schaeffter T, Razavi R, Hurtado DE, Uribe S, Figueroa CA. Pressure gradient prediction in aortic coarctation using a computational-fluid-dynamics model: validation against invasive pressure catheterization at rest and pharmacological stress. *J Cardiovasc Magn Reson*. 2015;17:Q78.

133. Wildermuth S, Dumoulin CL, Pfammatter T, Maier SE, Hofmann E, Debatin JF. MR-guided percutaneous angioplasty: assessment of tracking safety, catheter handling and functionality. *Cardiovasc Intervent Radiol*. 1998;21:404–410.

134. Yang X, Atalar E. Intravascular MR imaging-guided balloon angioplasty with an MR imaging guide wire: feasibility study in rabbits. *Radiology*. 2000;217:501–506.

135. Yang X, Bolster BD, Kraitchman DL, Atalar E. Intravascular MR-monitored balloon angioplasty: an in vivo feasibility study. *JVIR*. 1998;9:953–959.

136. Godart F, Beregi JP, Nicol L, Occelli B, Vincentelli A, Daanen V, Rey C, Rousseau J. MR-guided balloon angioplasty of stenosed aorta: in vivo evaluation using near-standard instruments and a passive tracking technique. *J Magn Reson Imaging*. 2000;12:639–644.

137. Omary RA, Frayne R, Unal O, Warner T, Korosec FR, Mistretta CA, Strother CM, Grist TM. MR-guided angioplasty of renal artery stenosis in a pig model: a feasibility study. *JVIR*. 2000;11:373–381.

138. Krueger JJ, Ewert P, Yilmaz S, Gelernter D, Peters B, Pietzner K, Bornstedt A, Schnackenburg B, Abdul-Khaliq H, Fleck E, Nagel E, Berger F, Kuehne T. Magnetic resonance imaging-guided balloon angioplasty of coarctation of the aorta: a pilot study. *Circulation*. 2006;113:1093–1100.

139. Kuehne T, Weiss S, Brinkert F, Weil J, Yilmaz S, Schmitt B, Ewert P, Lange P, Gutberlet M. Catheter visualization with resonant markers at MR imaging-guided deployment of endovascular stents in swine. *Radiology*. 2004;233:774–780.

140. Kuehne T, Saeed M, Higgins CB, Gleason K, Krombach GA, Weber OM, Martin AJ, Turner D, Teitel D, Moore P. Endovascular stents in pulmonary valve and artery in swine: feasibility study of MR imaging-guided deployment and postinterventional assessment. *Radiology*. 2003;226:475–481.

141. Raval AN, Telep JD, Guttman MA, Ozturk C, Jones M, Thompson RB, Wright VJ, Schenke WH, DeSilva R, Aviles RJ, Raman VK, Slack MC, Lederman RJ. Real-time magnetic resonance imaging-guided stenting of aortic coarctation with commercially available catheter devices in Swine. *Circulation*. 2005;112:699–706.

142. Buecker A, Neuerburg JM, Adam GB, Glowinski A, Schaeffter T, Rasche V, Van Vaals JJ, Molgaard-Nielsen A, Guenther RW. Real-time MR fluoroscopy for MR-guided iliac artery stent placement. *J Magn Reson Imaging*. 2000;12:616–622.

143. Quick HH, Kuehl H, Kaiser G, Bosk S, Debatin JF, Ladd ME. Inductively coupled stent antennas in MRI. *Magn Reson Med*. 2002;48:781–790.

144. Arepally A, Karmarkar PV, Weiss C, Rodriguez ER, Lederman RJ, Atalar E. Magnetic resonance image-guided trans-septal puncture in a swine heart. *J Magn Reson Imaging*. 2005;21:463–467.

145. Raval AN, Karmarkar PV, Guttman MA, Ozturk C, DeSilva R, Aviles RJ, Wright VJ, Schenke WH, Atalar E, McVeigh ER, Lederman RJ. Real-time MRI guided atrial septal puncture and balloon septostomy in swine. *Cathet Cardiovasc Intervent*.

2006;67:637–643.

146. Buecker A, Spuentrup E, Grabitz R, Freudenthal F, Muehler EG, Schaeffter T, van Vaals JJ, Günther RW. Magnetic resonance-guided placement of atrial septal closure device in animal model of patent foramen ovale. *Circulation*. 2002;106:511–515.

147. Rickers C, Jerosch-Herold M, Hu X, Murthy N, Wang X, Kong H, Seethamraju RT, Weil J, Wilke NM. Magnetic resonance image-guided transcatheter closure of atrial septal defects. *Circulation*. 2003;107:132–138.

148. Schalla S, Saeed M, Higgins CB, Martin A, Weber O, Moore P. Magnetic resonance--guided cardiac catheterization in a swine model of atrial septal defect. *Circulation*. 2003;108:1865–1870.

149. Schalla S, Saeed M, Higgins CB, Weber O, Martin A, Moore P. Balloon sizing and transcatheter closure of acute atrial septal defects guided by magnetic resonance fluoroscopy: assessment and validation in a large animal model. *J Magn Reson Imaging*. 2005;21:204–211.

150. Kuehne T, Yilmaz S, Meinus C, Moore P, Saeed M, Weber O, Higgins CB, Blank T, Elsaesser E, Schnackenburg B, Ewert P, Lange PE, Nagel E. Magnetic resonance imaging-guided transcatheter implantation of a prosthetic valve in aortic valve position: Feasibility study in swine. *JAC*. 2004;44:2247–2249.

151. Spuentrup E, Ruebben A, Schaeffter T, Manning WJ, Günther RW, Buecker A. Magnetic resonance--guided coronary artery stent placement in a swine model. *Circulation*. 2002;105:874–879.

152. Zhang S, Rafie S, Chen Y, Hillenbrand CM, Wacker FK, Duerk JL, Lewin JS. In vivo cardiovascular catheterization under real-time MRI guidance. *J Magn Reson Imaging*. 2006;24:914–917.

153. Serfaty JM, Yang X, Aksit P, Quick HH, Solaiyappan M, Atalar E. Toward MRI-guided coronary catheterization: visualization of guiding catheters, guidewires, and anatomy in real time. *J Magn Reson Imaging*. 2000;12:590–594.

154. Serfaty J-M, Yang X, Foo TK, Kumar A, Derbyshire A, Atalar E. MRI-guided coronary catheterization and PTCA: A feasibility study on a dog model. *Magn Reson Med*. 2003;49:258–263.

155. Ratnayaka K, Raman VK, Faranesh AZ, Sonmez M, Kim J-H, Gutiérrez LF, Ozturk C, McVeigh ER, Slack MC, Lederman RJ. Antegrade percutaneous closure of membranous ventricular septal defect using X-ray fused with magnetic resonance imaging. *JACC Cardiovasc Interv*. 2009;2:224–230.

156. Ratnayaka K, Rogers T, Schenke W, Mazal JR. Transcatheter bidirectional Glenn shunt guided by real-time MRI. *Journal of …*. 2015;

157. Dick AJ, Guttman MA, Raman VK, Peters DC, Pessanha BSS, Hill JM, Smith S, Scott G, McVeigh ER, Lederman RJ. Magnetic resonance fluoroscopy allows targeted delivery of mesenchymal stem cells to infarct borders in Swine. *Circulation*. 2003;108:2899–2904.

158. Dick AJ, Lederman RJ. MRI-guided myocardial cell therapy. *Int J Cardiovasc Intervent*. 2005;7:165–170.

159. de Silva R, Gutiérrez LF, Raval AN, McVeigh ER, Ozturk C, Lederman RJ. X-ray fused with magnetic resonance imaging (XFM) to target endomyocardial injections: validation in a swine model of myocardial infarction. *Circulation*. 2006;114:2342–2350.

160. McVeigh ER, Guttman MA, Lederman RJ, Li M, Kocaturk O, Hunt T, Kozlov S, Horvath KA. Real-time interactive MRI-guided cardiac surgery: aortic valve replacement using a direct apical approach. *Magn Reson Med*. 2006;56:958–964.

161. Yang X, Atalar E. MRI-guided gene therapy. *FEBS Lett*. 2006;580:2958–2961.

162. Bennett MK, Gilotra NA, Harrington C, Rao S, Dunn JM, Freitag TB, Halushka MK, Russell SD. Evaluation of the role of endomyocardial biopsy in 851 patients with unexplained heart failure from 2000-2009. *Circ Heart Fail*. 2013;6:676–684.

163. Lardo AC, McVeigh ER, Jumrussirikul P, Berger RD, Calkins H, Lima J, Halperin HR. Visualization and temporal/spatial characterization of cardiac radiofrequency ablation lesions using magnetic resonance imaging. *Circulation*. 2000;102:698–705.

164. Nordbeck P, Bauer WR, Fidler F, Warmuth M, Hiller KH, Nahrendorf M, Maxfield M, Wurtz S, Geistert W, Broscheit J, Jakob PM, Ritter O. Feasibility of Real-Time MRI With a Novel Carbon Catheter for Interventional Electrophysiology. *Circ Arrhythm Electrophysiol*. 2009;2:258–267.

165. Nazarian S, Kolandaivelu A, Zviman MM, Meininger GR, Kato R, Susil RC, Roguin A, Dickfeld TL, Ashikaga H, Calkins H, Berger RD, Bluemke DA, Lardo AC, Halperin HR. Feasibility of real-time magnetic resonance imaging for catheter guidance in electrophysiology studies. *Circulation*. 2008;118:223–229.

166. Griffin GH, Anderson KJT, Celik H, Wright GA. Safely assessing radiofrequency heating potential of conductive devices using image-based current measurements. *Magn Reson Med*. 2015;73:427–441.

FIGURE LEGENDS

Figure 1: Images from a rotational angiogram overlayed onto X-ray fluoroscopy during percutaneous pulmonary valve implantation. In figure 1a, the image overlay appears good. During

deployment of the valve, the use of a stiff wire distorts the anatomy of the right ventricular outflow tract and the previously acquired 3D angiogram is no longer in line with the fluoroscopic image.

Figure 2 XMR room with the X-ray and MR equipment joined by a movable tabletop. The c-arm of the X-ray unit is seen in the foreground, ceiling-mounted MR monitor and controls are seen in the distance, and the 5-gauss area is demarcated by a change in the floor colouring from the MR to the X-ray end of the room.

Figure 3 Passive tracking. Inflated balloon angiographic Bermann catheter filled with 0.8 mL CO_2 from the inferior vena cava to the right pulmonary artery using solely magnetic resonance guidance. *Arrows* show the signal void of the catheter tip as it traverses the inferior vena cava, right atrium, tricuspid valve, and right ventricular outflow tract and enters the pulmonary artery.

Figure 4 PSat sequence guidance of a catheter filled with gadolinium in the inferior vena cava of a patient with a cavopulmonary connection. The gadolinium filled tip appears bright white on this image.

Figure 5 X-ray and magnetic resonance intervention. 5a. Patient is placed on the magnetic resonance tabletop on the X-ray half of the room for sheath insertion. The MRI coils are demonstrated inset. 5b Image artefact from MRI coils on X-ray fluoroscopy. 5c. Patient is slid into the MRI scanner for MRI guided catheterisation. 5d. Image of foot pedals for in-room manipulation of the imaging planes by the primary operator.

Figure 6 Schematic of the history of MRI catheterisation in humans and animals. Boxes marked in red relate to human studies. Boxes marked white relate to animal studies.

Figure 7 CMR-guided EP platform during clinical ablation of atrial flutter using active tracking (iSuite, Philips Research, Hamburg). All four panels are demonstrated simultaneously to the electrophysiology operator. The two left hand panels show orthogonal reconstructions of a b-SSFP 3D dataset (multiplanar reconstruction (MPR) 1 and 2). Location of prior ablation lesions are shown as red dots. Ablation catheter icon is red, and diagnostic/pacing catheter in green. The upper right hand panel is a single frame of a cine acquisition acquired a few seconds before, automatically oriented along the shaft of the ablation catheter, demonstrating the ablation catheter position. The lower right hand panel shows a close-up of the right atrial shell and the locations of the ablation lesions. Colour-coding is according to the timing of atrial activation on mapping whilst pacing from the coronary sinus, with earliest activation shown in red.

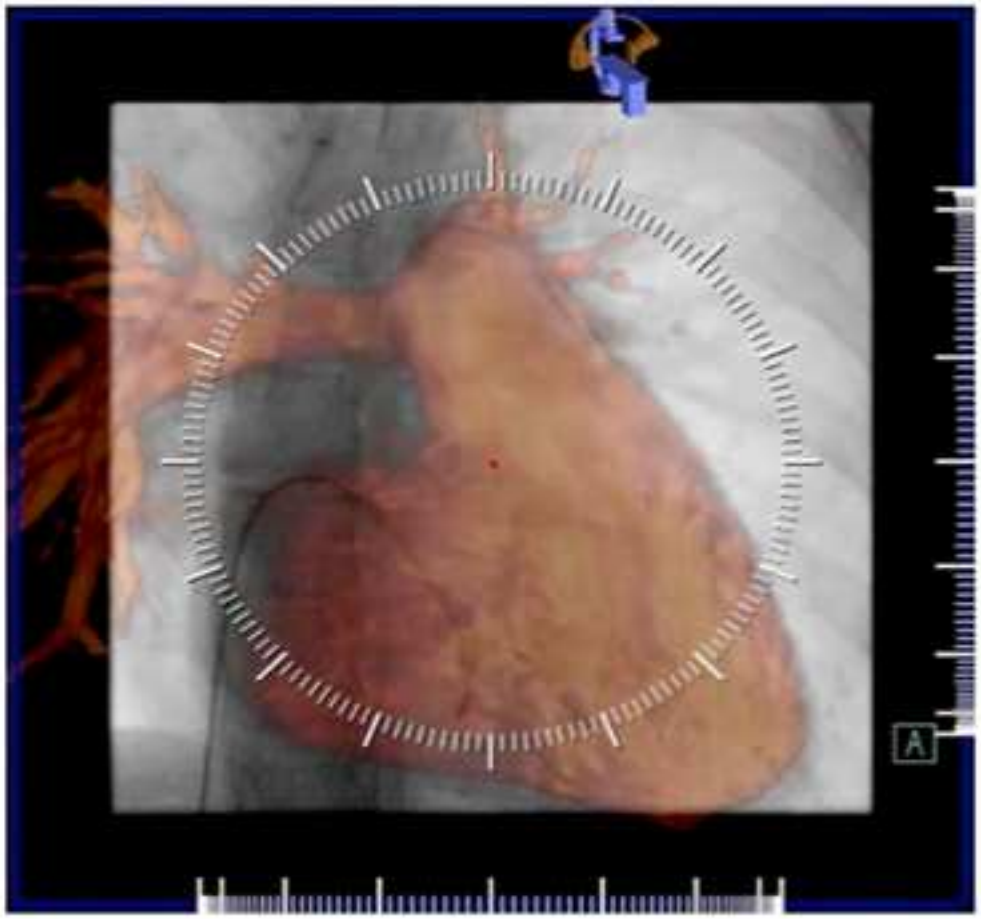

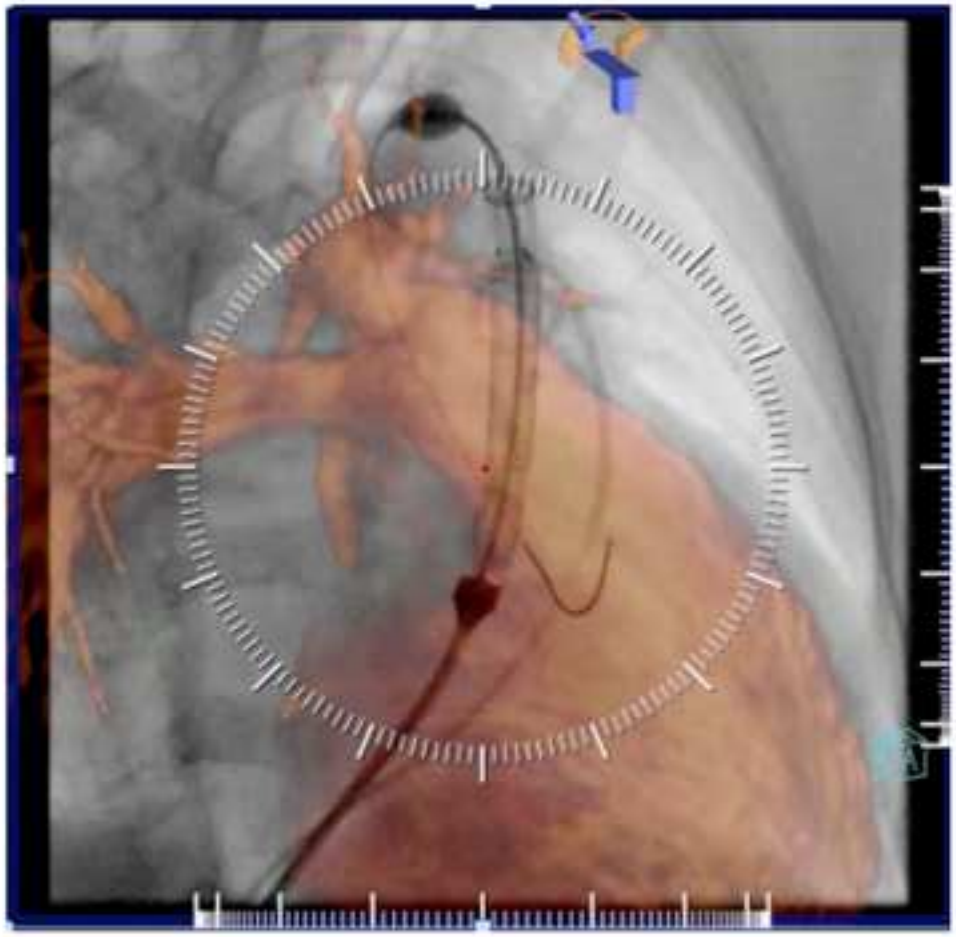

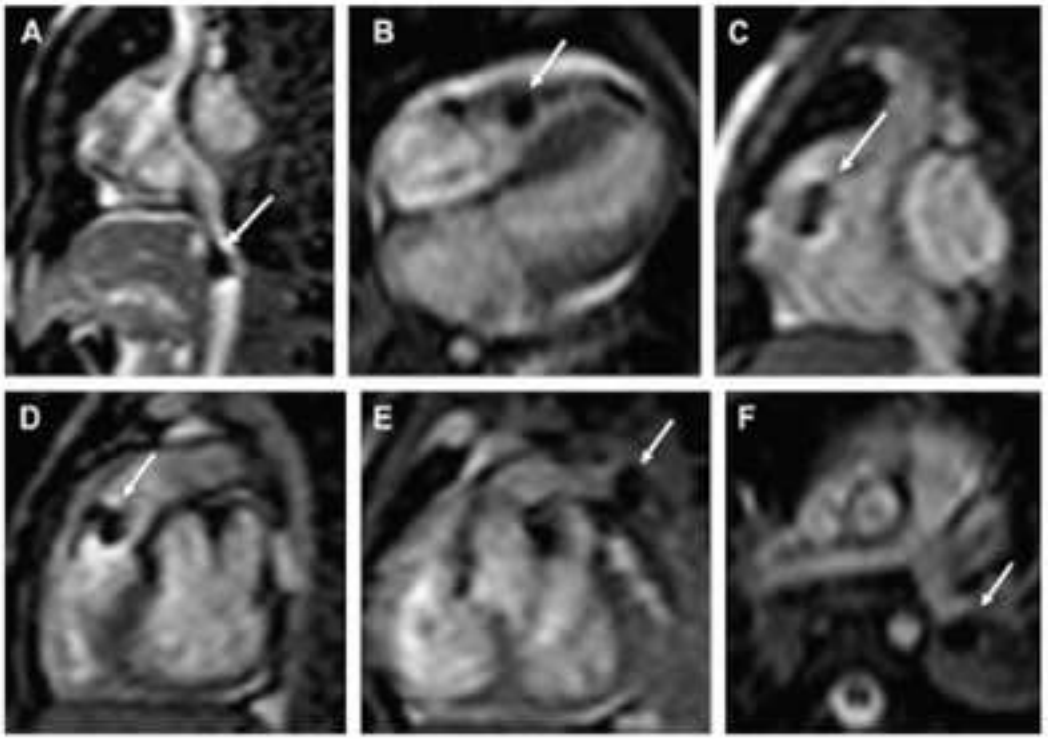

Manuscript (All Manuscript Text Pages, including Title Page, References and Figure Legends)

Click here to download Manuscript (All Manuscript Text Pages, including Title Page, References and Figure Legends) Figure 5a.tif

Manuscript (All Manuscript Text Pages, including Title Page, References and Figure Legends)

Click here to download Manuscript (All Manuscript Text Pages, including Title Page, References and Figure Legends) Figure 5b.tif

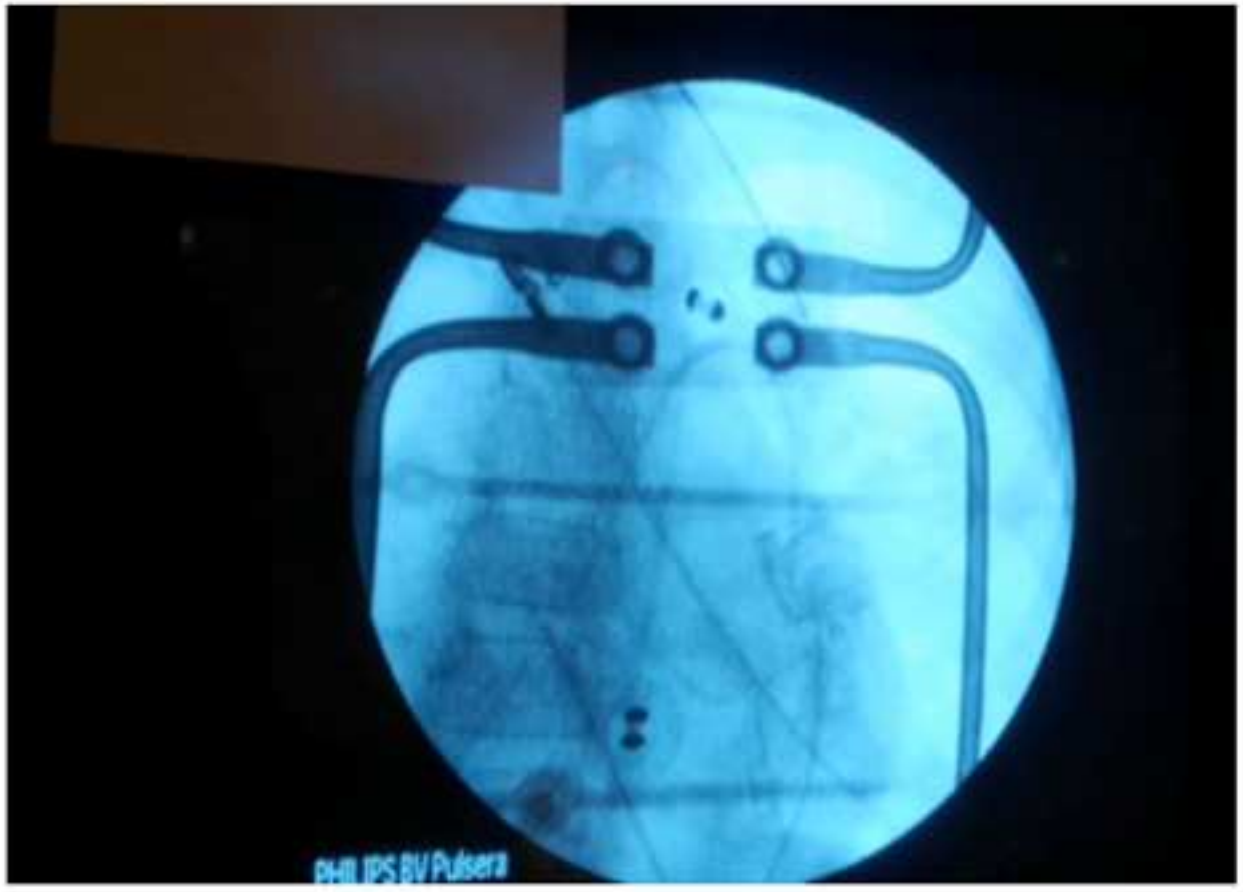

Manuscript (All Manuscript Text Pages, including Title Page, References and Figure Legends)

Click here to download Manuscript (All Manuscript Text Pages, including Title Page, References and Figure Legends) Figure 5c.tif

Manuscript (All Manuscript Text Pages, including Title Page, References and Figure Legends)

Click here to download Manuscript (All Manuscript Text Pages, including Title Page, References and Figure Legends) Figure 5d.tif